On the possibilities of the orbital asymmetry of the Karin family

Ireneusz Wlodarczyk[1], Jacek Leliwa-Kopystynski[2]
[1] Chorzow Astronomical Observatory, 41-500 Chorzow, Poland
[2] University of Warsaw, Institute of Geophysics, Pasteura 7, 02-093 Warsaw, Poland
jkopyst@mimuw.edu.pl
(Submitted on 23.03.2026; Accepted on 16.06.2026)

Ireneusz Wlodarczyk passed away on March 11, 2026.

Abstract. In this work, we compare the real family of Karin with six synthetic families formed from clones ejected from six points on the surface of the parent body, which were oriented differently to the Sun and Karin's orbit. We found that the orbital parameter distributions of members of these clone-formed families differ significantly from those of the real Karin family members. Unfortunately, a clone-formed family that would match the actual Karin family were not found.

1. Introduction

It is commonly accepted that most asteroid families (AFs) were formed by impacts on the parent bodies (PBs). Choosing the members of an asteroid family (AFMs) is performed using the Hierarchical Clustering Method (HCM) developed by Zappalà et al. ([Zappala et al., 1990]), and afterwards improved by many researchers. The HCM should be assisted by auxiliary methods that will eliminate from the potential collection of the AFMs interlopers, that is, asteroids not genetically connected to the primordial impacted body. Let, for a given AF, a set of AFMs be already found. This means that the orbital elements (a, e, i) of all AFMs are known. The AF considered in this work will be the Karin family, the youngest one known to date. Nesvorný et al. ([Nesvorny et al., 2002, Nesvorny et al., 2006]) estimated that the age of the Karin family is only about (5.8 ± 0.2) million years. So, it can be expected that the Karin family members (FMs) only slightly changed their orbital elements from the moment of the family formation. We focus our attention on the distribution of the orbital elements of the clones-formed AFMs relative to the orbital elements of Karin. Histograms are prepared for the 1086 FMs of the Karin family, previously considered by Leliwa-Kopystynski & Wlodarczyk ([Leliwa-Kopystynski and Wlodarczyk, 2024]). It is noteworthy that the histograms are highly nonsymmetrical versus a, e, and i of Karin.

2. Formulation of the problem

In this section, we consider the orbital fate of the post-impact ejecta kicked out of the surface of a PB in dependence on their initial velocity and their initial direction. The asteroid that threw out the ejecta (the clones) was the real PB of the present AF. Our choice of the real family is the Karin family, the youngest known. We consider the three-body system composed of the Sun, the PB, and a massless post-impact fragment. The model is three-dimensional as the clones are thrown away from the PB, forming the ejecta cone. We are interested in the orbital parameters of the clones while they are far enough from the PB, therefore, beyond its Hill sphere. The perturbations of the clones' orbits by the planets are not considered. We are considering several variants of asteroid family formation. We are looking for a family formed of clones that will be most similar to the real family (here, the Karin family).

Let the PB be an asteroid with the mass M, the radius R, the semiaxis a, and the mean orbital velocity v_{orb}. There are two values of the escape velocity v_{es} involved in our considerations. They are the escape velocity $v_{es,PB}$ from the surface of the asteroid PB, and the escape velocity $v_{es,a}$ from the circumsolar orbit of the PB:

$$v_{es,PB} = \sqrt{\frac{2GM}{R}} \tag{1}$$

$$v_{es,a} = \sqrt{2}\, v_{orb} \tag{2}$$

Here, the gravity constant is $G = 6.6743 \times 10^{-11}\,\mathrm{m^3\,kg^{-1}\,s^{-2}}$. For any potential PB, the escape velocity $v_{es,PB}$, is at most a few dozen meters per second. It is worth noting that the escape velocity is quite well approximated by the rule that $v_{es,PB}$ expressed in meters per second, is equal to the radius of the PB expressed in kilometres. Thus, for the Karin as well as for the PB of the Karin family, both having radii ∼10 km, the escape velocity is about 10 m/s. The collisional velocities of the asteroids in the main belt are ∼5 km/s ([Cibulkova et al., 2014]). The orbital velocities v of the PBs are within the range of 15–20 km/s and thus $v_{es,a} \approx$ (20–30) km/s. None or only a very few fragments resulting from the collision could have reached a speed exceeding the value of $v_{es,a}$. Thus, all the fragments, even the fastest, must remain in the main belt and orbit the Sun.

The fragments ejected from the surface of the PB are subject to the gravity of the PB and the Sun. The gravity of the PB prevails inside the Hill region, the radius of which is given by the following approximate formula:

$$r_{\mathrm{Hill}} = a_{\mathrm{PB}} \left(\frac{M_{\mathrm{PB}}}{3M_{\odot}} \right)^{1/3} \tag{3}$$

The ejected fragment escapes from the gravity-dominated region of the PB after a time interval t_{eject} that is approximately equal to $r_{\mathrm{Hill}}/v_{eject}$, where v_{eject} is its ejection velocity from the PB surface, relative to the point of ejection. After a few intervals of time, each equal to t_{eject}, the parameters of the circumsolar orbits of clones can be considered fixed. Using the data collected in Tab. 1, we estimate $t_{eject} \approx (r_{\mathrm{Hill}}/v_{eject}) \approx$ (5000 km / 50 m s-1) ≈ 1 day. The value $v_{eject} = 50\ \mathrm{m\,s^{-1}}$ corresponds to the reasonably adopted value of the speed of the set of a few hundred largest post-impact fragments, that is, those fragments that formed a family. From laboratory impact experiments, it is well known that larger fragments escape more slowly from PB than the smaller ones. Concluding, a time interval for considering the calculated orbital elements of the clones as definitive should last a few days. In our case, the calculations of the orbital parameters of each of the clones were interrupted after 5.79 days since the impact. After this time interval, the clones are sufficiently far away from the Hill limit of the PB, and the PB's gravitational influence on the clones' orbit is negligible.

Parameter	Adopted value
Semi-axis of Karin's orbit	2.8638 au
Mass of Karin	6.971×10^{15} kg
Mass of PB of Karin	1.278×10^{16} kg
Population of the Karin family	1086
Radius of Karin	8500 m
Radius of the PB of Karin	10404 m
Escape velocity from the surface of Karin	10.46 m/s
Escape velocity from the surface of PB of Karin	12.54 m/s
Hill radius for Karin	4510 km
Hill radius for the PB of Karin	5520 km
Mean orbital velocity of Karin	17.59 km/s

Table 1: Physical parameters adopted for calculations. Values are taken from Tab. 2 of JLK & IW ([Leliwa-Kopystynski and Wlodarczyk, 2024]) or calculated from the data listed there.

3. Geometrical and orbital conditions

In reality, each collisional AF was created by an impact on any point of the surface of PB, while PB was at any point in its orbit. However, in our simulations, we study several cases of the clone-formed families where the impacted PB was in perihelion or in aphelion. Moreover, an impact occurred on one of the six cotes of the PB, differently oriented from the Sun-PB direction. We calculate the orbital parameters of all artificial AFMs (the clones) formed by impact on the true PB (here, the PB of Karin). Next, we construct histograms of the orbital parameters of the clones that formed an artificial family. They are the histograms of the semiaxes a, the eccentricities e, and the inclinations of the orbits i. Next, we compare them with those of the actual AF formed around this PB.

At first, we considered an AF consisting of 1086 clones, which is as large as Karin's actual family. An example of the comparison of the histograms of artificial AF containing 1086 clones with those formed of only 500 clones is presented in Fig. 2. The similarity of histograms for 1086 and 500 clones allows us to limit the number of clones to 500 in the following calculations.

As mentioned, although the creation of a true AF can be the result of an impact on any point of the PB occurring at any point of its orbit, our study restricts the impact scenarios to perihelion and aphelion. Of course, the position of the impact point on the PB where the actual AF was created, vs the actual orientation of the PB to the Sun, and the direction of the orbital movement of the PB, is unknown. It can be expected that the post-impact ejecta produced in the forward hemisphere of the PB should have, on average, the velocity component along the direction of the movement of PB on its orbit larger than the post-impact ejecta produced in the backwards hemisphere. Consequently, it can be expected that the clones' families produced from an impact on the same PB have slightly different ensembles of the orbital parameters.

The orbital parameters of all members of an AF consisting of clones depend at least on three factors presented below.

1. ***Geometric constraints.*** Let us consider the six geometrical possibilities of throwing out the ejecta from the PB. They will form the AF. In the considered cases, all ejecta (clones) start from one of the following surfaces:
   - the leading surface (LP),
   - the trailing surface (TP),
   - the sub-solar surface (SS),
   - the anti-sub-solar surface (AS),
   - the surface above the orbital plane of the PB (AOP),
   - the surface below the orbital plane of the PB (BOP).

   Geometrically, this model approximates the PB by a cube properly oriented relative to the Sun–PB line and the PB orbit. It can be expected that the distribution of the orbital parameters of the newly born AF depends on the orientation (relative to the Sun and the PB orbit) of the radius of PB that is going from the centre to the point where an impactor hits the PB surface. It can also be expected that the distribution depends on the impact angle of the impactor falling on the PB. However, the impact angle is not included in our model. We only assumed that the clones escape in random directions within the half-sphere above the starting point. Their initial escaping trajectories, relative to the PB, depend on three parameters. They are the azimuthal angle (0, 2π), the launch angle (0, $\pi/2$), and the launch speed v. For each ejected fragment, the angles were chosen randomly.
2. ***Launch speed v of ejecta relative to the starting point*** on the surface of PB. Their minimum value should be higher than the escape velocity $v_{es,PB}$ from PB. In this study, the velocity distribution of ejecta is not included in our model. This can be justified, following Cellino et al. ([Cellino et al., 1999]), who have found that ejection velocity scales as the size of a fragment to the power of the range (-1, -2/3). Most of the fragments forming an observable family have sizes of about (2 - 4) km, and therefore, their escape velocities differ by a term not larger than 2. That justifies an assumption adopted in this paper, that all ejecta forming the future family are composed of clones starting with the same speed (here v = 30 m/s, while $v_{es,PB} \approx 12$ m/s for the PB of Karin). This is a crude but acceptable approximation.
3. ***Position of the PB in the orbit at the moment of an impact*** and therefore at the moment of creation of an AF. The most visible differences among the ensembles of orbital parameters of the AFs can be expected when the creation of the clone family happens at opposite ends of the PB orbit, at perihelion or at aphelion. We checked that for the case of Karin's orbit Here, with only one exception, we consider creation in perihelion.

4. Results

We follow the orbital fate of the clones. That means we calculate the orbital elements of the clones $a(t)$, $e(t)$, and $i(t)$, step by step, at consecutive time moments. The calculations are stopped when the distance of a clone from the PB is greater than a few Hill's radii of the PB. From this moment, the orbits of the clones around the Sun are treated as fixed. We have examined the differences between the histograms of orbital elements for the families that originated from clones ejected from opposite points on the surfaces of the PB. Results are gathered in Figs. 3-6, where the orbital parameters of the families formed by 500 clones ejected from the opposite sides of the PB are presented in the histograms. Tab. 2 shows how the clones' orbital parameters are distributed relative to those of the actual Karin.

Semiaxis Left / Right	**Eccentricity Left / Right**	**Inclination Left / Right**	**Starting point on the PB**	**Starting point on the orbit of PB**	**Illustrated in Fig.**
320 / 766	286 / 800	470 / 616	1086 members of Karin's family. Starting point unknown	Unknown	Fig. 1
557 / 529 257 / 243	560 / 526 258 / 242	1033 / 53 477 / 23	1086 clones, AOP 500 clones, AOP	Perihelion	Fig. 2
229 / 271 271 / 229	227 / 273 229 / 271	368 / 132 249 / 251	SS SS	Perihelion Aphelion	Fig. 3
247 / 253 257 / 243	247 / 253 258 / 242	23 / 477 477 / 23	BOP AOP	Perihelion	Fig. 4
229 / 271 271 / 229	227 / 273 271 / 229	368 / 132 248 / 252	SS AS	Perihelion	Fig. 5
284 / 216 205 / 295	285 / 215 208 / 292	484 / 16 14 / 486	LP TP	Perihelion	Fig. 6

Table 2: Summary of the results presented in figures. The starting speed of clones, 30 m/s, is assumed throughout the whole text. Left / Right denotes the numbers of the differences $(a — a_{Karin})$, or $(e — e_{Karin})$, or $(i — i_{Karin})$, negative or positive, respectively, regarding the values a, e, i of Karin. Clones' families were formed while PB was in perihelion, except for one case.

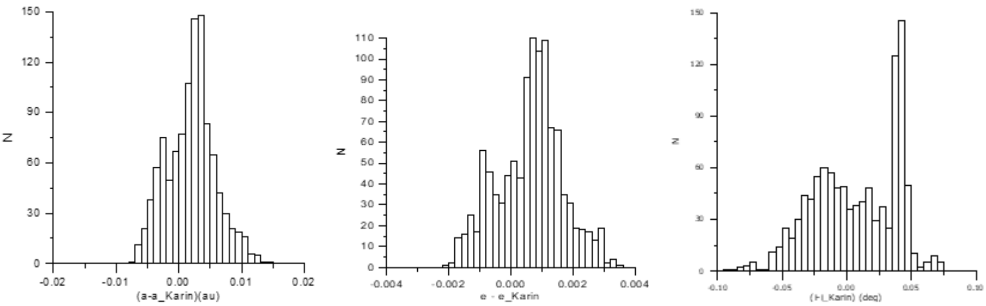

(a) Semiaxis distribution (b) Eccentricity distribution (c) Inclination distribution

Fig. 1: Distribution of the orbital parameters of the Karin FMs vs the orbital parameters of Karin.

Comparison of orbital parameters for clone families formed in perihelion versus those formed in aphelion is presented in one case, as shown in Fig. 3. The histograms in the left column of Fig. 3 (perihelion) differ substantially from those in the right column (aphelion). In particular, differences are the strongest for distributions of family members vs their inclinations.

Figs. 4-6 illustrate the differences among the histograms of the clones' families that have been formed from fragments ejected on opposite sides of PB.

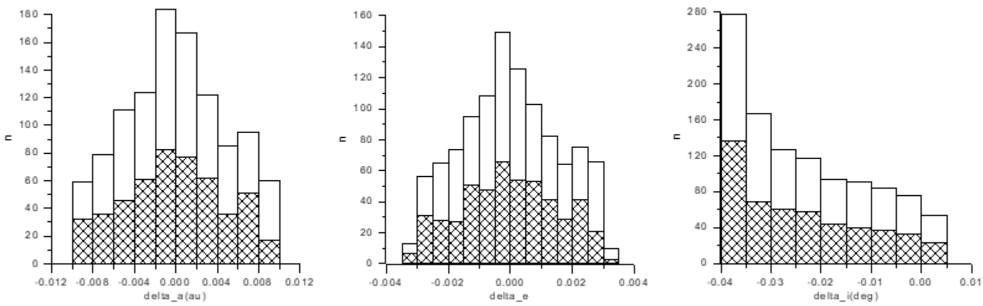

(a) Semiaxis distribution (b) Eccentricity distribution (c) Inclination distribution

Fig. 2: Clones start from perihelion, Above Orbital Plane (AOP). Upper contours are for 1086 clones, and lower contours are for 500 clones.

Comparison of histograms for the cases of formation of AF by ejecta escaped from the points BOB and AOP, Fig. 4. The histograms for Δa and Δe are rather similar. However, the histograms for Δi differ significantly from each other.

Comparison of histograms for the cases of formation of AF by ejecta escaped from the points SS and AS, Fig. 5.

Comparison of histograms for the cases of formation of AF by ejecta escaped from the points LP and TP, Fig. 6.

5. Conclusions

1. The shape of the ejecta swarm (in a, e, i space) depends strongly on the actual orientation of the point on the surface of PB from which the clones are ejected.
2. Regardless of the point on the surface of PB from which the clones are ejected, the histograms of the inclination of the clones' orbits show a tendency to disperse out of the orbital plane of PB, Figs. 3-6.
3. Within the scope of this work, it is not possible to determine from which area of the PB the ejecta that formed the AF was thrown, since the rotation of the PB is not taken into account. Additionally, the limited knowledge about the surface features of Karin ([Sasaki et al., 2004,Sasaki et al., 2006]) is insufficient to determine the position from which the ejecta was thrown. In this work, the speed of the ejecta was a free parameter; it was set to 30 m/s. It would be useful to introduce the ejecta velocity distribution vs their size distribution. However, such an enlargement requires introducing additional parameters.

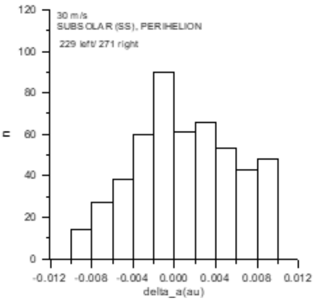

(a) Perihelion: Δa

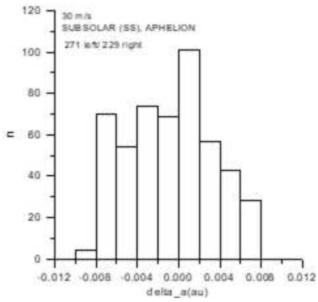

(b) Aphelion: Δa

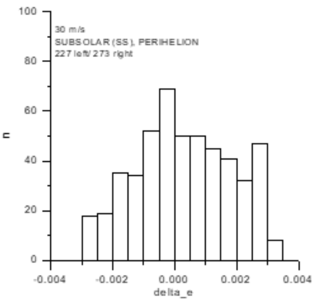

(c) Perihelion: Δe

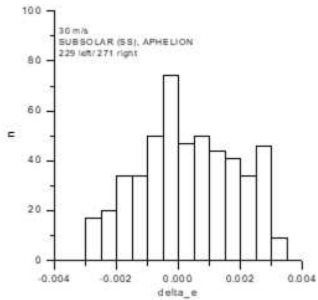

(d) Aphelion: Δe

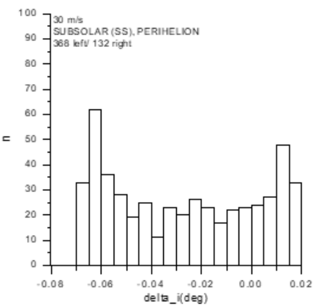

(e) Perihelion: Δi

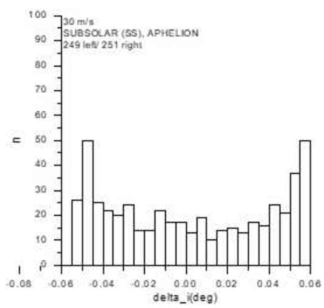

(f) Aphelion: Δi

Fig. 3: The 500 clones started from the Sub-Solar point (SS) while the PB was in perihelion (left column), and aphelion (right column). The distributions of the orbital elements are shown for Δa, Δe, and Δi.

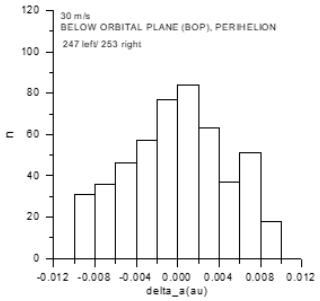

(a) BOB: Δa

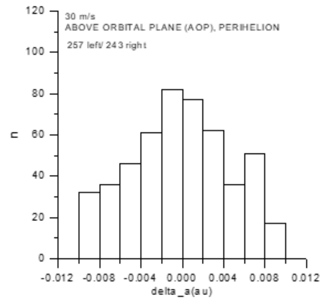

(b) AOP: Δa

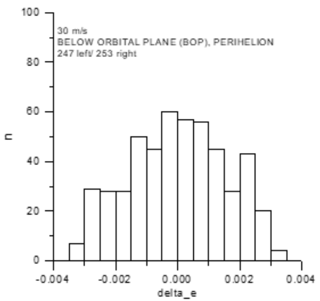

(c) BOB: Δe

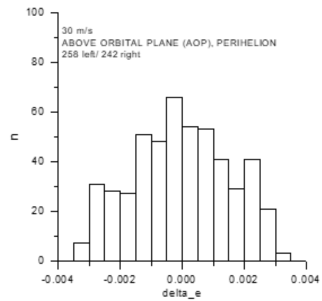

(d) AOP: Δe

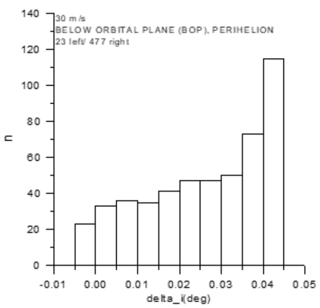

(e) BOB: Δi

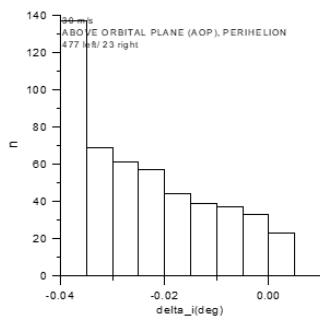

(f) AOP: Δi

Fig. 4: Comparison of histograms for the cases of formation of AF by ejecta escaped from the points Below the Orbital Plane (BOB) and Above the Orbital Plane (AOP). This figure is the compilation of the left column of Fig. 3 with the shadowed part of Fig. 2.

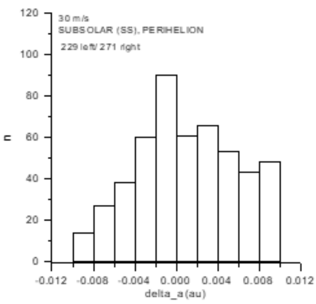

(a) SS: Δa

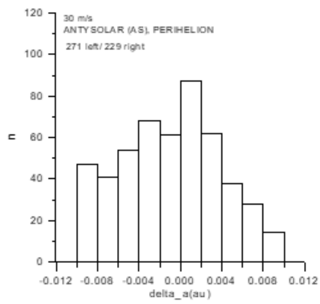

(b) AS: Δa

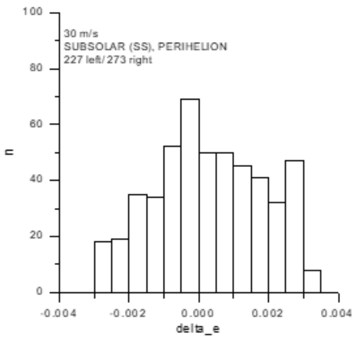

(c) SS: Δe

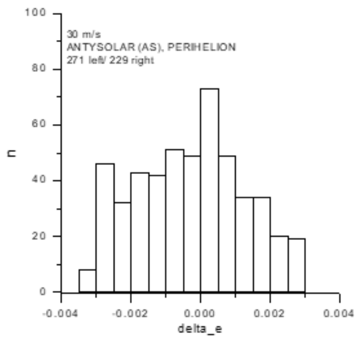

(d) AS: Δe

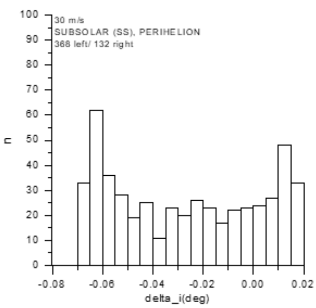

(e) SS: Δi

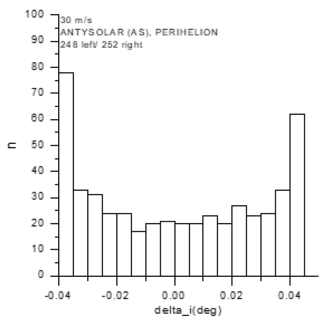

(f) AS: Δi

Fig. 5: 500 clones were started from the Sub-Solar point (SS, left column), and the Anti-Solar point (AS, right column) while the PB was in perihelion.

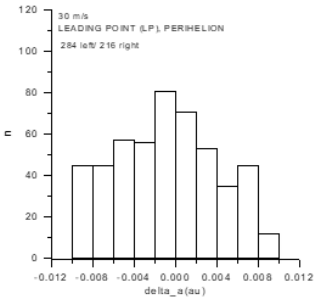

(a) LP: Δa

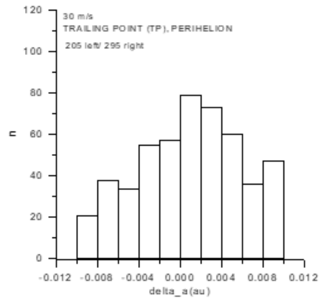

(b) TP: Δa

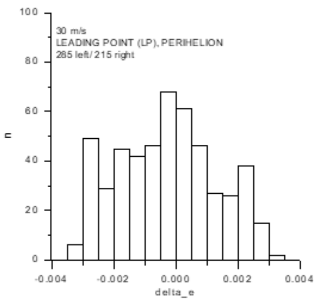

(c) LP: Δe

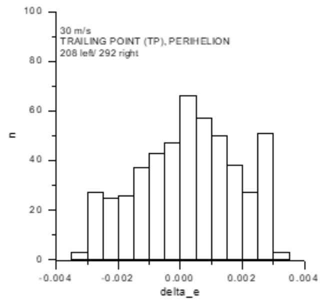

(d) TP: Δe

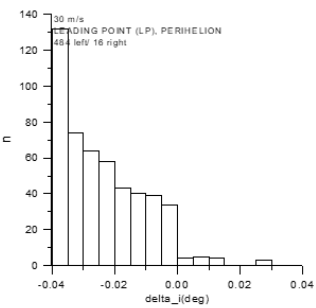

(e) LP: Δi

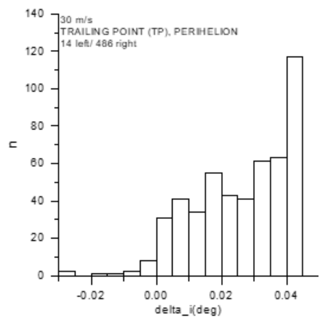

(f) TP: Δi

Fig. 6: 500 clones were started from the Leading Point (LP, left column), or the Trailing Point (TP), while the PB was in perihelion.

References

Cellino, A., Michel, P., Tanga, V., Zappala, P., Paolicchi, A., and Dell'Oro, A. (1999). The velocity–size relationship for members of asteroid families and implications for the physics of catastrophic collisions. *Icarus*, 141(1):79–95.

Cibulkova, H., Broz, M., and Benavidez, P. G. (2014). A six-part collisional model of the main asteroid belt. *Icarus*, 241:358–372.

Leliwa-Kopystynski, J. and Wlodarczyk, I. (2024). The minimal sizes of impactors that formed the vesta family and 15 other asteroid families. *Monthly Notices of the Royal Astronomical Society*, 528(4):6312–6318.

Nesvorny, D., Bottke, W. F. J., Dones, L., and Levison, H. F. (2002). The recent breakup of an asteroid in the main-belt region. *Nature*, 417(6890):720–722.

Nesvorny, D., Enke, B. L., Bottke, W. F., Durda, D. D., Asphaug, E., and Richardson, D. C. (2006). Karin cluster formation by asteroid impact. *Icarus*, 183(2):296–311.

Sasaki, S., Sasaki, T., Watanabe, J.-i., Yoshida, F., Kawakita, H., Takato, N., Dermawan, B., Fuse, T., Ito, T., and Sekiguchi, T. (2006). A newborn asteroid 832 karin with old and new surfaces – subaru spectroscopy. *Advances in Space Research*, 38(9):1995–1999.

Sasaki, T., Sasaki, S., Watanabe, J.-i., Sekiguchi, T., Kawakita, H., Fuse, T., Takato, N., Yoshida, F., Dermawan, B., and Ito, T. (2004). Mature and fresh surfaces on the newborn asteroid karin. *Astrophysical Journal*.

Zappala, V., Cellino, A., Farinella, P., and Knezevic, Z. (1990). Asteroid families. i: Identification by hierarchical clustering and reliability assessment. *Astrophysical Journal*, 100:2030.